

Alzwayi, A.S., and Paul, M.C. (2014) *Transition of free convection flow inside an inclined parallel walled channel: effects of inclination angle and width of the channel*. International Journal of Heat and Mass Transfer, 68 . pp. 194-202. ISSN 0017-9310

Copyright © 2014 Elsevier Ltd.

A copy can be downloaded for personal non-commercial research or study, without prior permission or charge

Content must not be changed in any way or reproduced in any format or medium without the formal permission of the copyright holder(s)

When referring to this work, full bibliographic details must be given

<http://eprints.gla.ac.uk/86904/>

Deposited on: 21 October 2013

TRANSITION OF FREE CONVECTION FLOW INSIDE AN INCLINED PARALLEL WALLED CHANNEL: EFFECTS OF INCLINATION ANGLE AND WIDTH OF THE CHANNEL

Ali S. Alzwayi¹ and Manosh C. Paul[§]

Systems, Power & Energy Research Division, School of Engineering, University of Glasgow,
Glasgow G12 8QQ, UK

[§]Corresponding author: Email: Manosh.Paul@glasgow.ac.uk, Tel: +44(0)141 330 8466, Fax:
+44(0)141 330 4343

ABSTRACT

Transition of free convection flow in an inclined parallel walled channel has been investigated numerically by employing $k-\epsilon$ turbulent model. Particular attention is paid on how the inclination angle and width of the channel affect the transition process of the flow developing in the channel. The upper plate of the channel is heated isothermally and facing downward, while the lower one is kept under the adiabatic condition. The inclination angle of the channel is varied from 0° to 85° with respect to its vertical position while the distance separating the two plates is systematically reduced from 0.45 m to 0.06 m. Distributions of velocity, turbulent kinetic energy and local heat flux are presented to examine the critical distance and the results obtained show good agreement with experimental data available in the literature.

KEYWORDS: Free convection; Channel inclination; Laminar flow; Transition; Critical distance; Turbulent flow; Heat transfer

¹On Study leave from the Department of Mechanical Engineering, Faculty of Engineering and Technology, Sabha University, P.O. Box 53808, Brak, Libya.

NOMENCLATURE

b	channel width
C_p	air specific heat capacity
g	gravitational acceleration
Gr	Grashof number = $g\beta(T_P - T_a)y^3/\nu^2$
h	heat transfer coefficient = $qp/(Tp - Ta)$
k	kinetic energy of turbulence
L	channel height
A	mass flow rate
Nu	average of Nusselt number = $h b/\kappa$
n_y, n_x	number of nodes in the y and x directions respectively
p, p_o	static and ambient pressure respectively
Pr	Prandtl number
q_p	heat flux of the plate = $\int \frac{\partial T}{\partial x} \Big _{x=0} dy$
Ra	Rayleigh number = $Gr Pr$
T	temperature
u, v	velocity components in the x and y directions respectively
x, y	Cartesian coordinates

Greek Symbols

α	angle of inclination with respect to the vertical direction
β	thermal expansion coefficient
ϵ	exchange coefficient for general transport defined as μ/Pr
ρ	density
ν	kinematic viscosity

μ	dissipation rate of turbulent kinetic energy
μ	dynamic viscosity coefficient
μ_t	turbulent molecular viscosity
\tilde{A}_t	turbulent Prandtl number
κ	thermal conductivity

Subscripts

a	air
P	plate
e	experimental
n	numerical
c	critical
in	inlet

1. ITRODUCTION

Natural convection in inclined parallel plates has received great attention in the recent years due to a wide range of engineering applications including solar energy systems. Particularly, in modern buildings sloped roofs, multi-glazed windows and skylights are frequently installed, and they are exposed to both free and forced convections. As far as the flow of free convection on a tilted plate is concerned, the first experiment was carried out by Rich [1953] in 1953. Average heat transfer rate along the heated plate at various angles up to 40° was measured. The experimental data indicated that the heat transfer drops when the heated plate is moved from its vertical position.

After about 3 decades, Azevedo and Sparrow [1985] performed a comprehensive experimental study of laminar free convection in an inclined isothermal channel. They investigated three heating models: heating from above, heating from below, and symmetric heating, where the channel was closed from both sides. The average of Nusselt number was evaluated in all the experimental conditions in the range 0° - 45° from the vertical position, and they reported the data in a global correlation with an average error of $\pm 10\%$. Later, Manca et al. [1992] followed this work and concerned the investigation of the Nusselt number with a uniform heat flux condition.

Onur et al. [1997] and Onur and Aktas [1998] provided experimental data of the effect of the inclination angle and width on developing heat transfer between inclined parallel plates with different heating conditions. In particular, Onur et al. [1997] considered the lower plate isothermally heated and the upper plate insulated, while in Onur and Aktas [1998] the upper plate was heated isothermally whereas the lower was insulated. The channel inclination was 0° , 30° and 45° with a range of Rayleigh number between 3×10^7 and 9×10^7 . The measurement was carried out for different temperatures of air and plate and the results indicated that both the inclination and width influence the heat transfer rate.

In the late 90s and more recently, numerous numerical papers on free convection have been published. Numerical investigation of the free convention in inclined channel carried out by

Baskaya et al. [1999] seems relevant to the work presented in this paper. However, they particularly focused on the laminar convection flow. Recently, two-dimensional turbulent natural convection flow inside an inclined parallel walled channel has been studied numerically by Said et al. [2005a, 2005b], where both the upper and lower plates were isothermal. A $k-\epsilon$ turbulent model (FLUENT code) was employed in the simulation and the results satisfactory agreed with Elenbaas [1942], Miyamoto et al. [1983], and Fedorov and Viskanta [1997]. Their results further indicated that the average of Nusselt number is reduced with an increase in the plate angle. However, the process of transition that occurs from laminar to turbulence was not considered in the study. In fact, all the papers cited above either considered laminar or turbulent flow and neglected the transition of developing free convection in an inclined channel. Most recently, Alzwayi and Paul [2013] have investigated numerically the transition of thermal boundary layer in a vertical parallel plate channel with an affect of its width and temperature.

In the context of a heated surface facing upward, Kierkus [1968], Lloyd and Sparrow [1970], Hassan and Mohamed [1970], Balck and Norris [1975] and AL- Arabi and Sakr [1988] studied the transition stage under different kinds of fluid and heating conditions. Recently, Paul et al. [2005] also looked into the effects of angle on the thermal boundary layer stability. However, very little information is available on the transition of flow on a heated surface facing downward. Hassan and Mohamed [1970] tried to investigate the transition of free convection flow for both the downward and upward facing heated surfaces but they were unable to get the transition point for the heated surface facing downward due to the short length of the plate. Even they could not get the transition stage in the vertical case because of the same reason. Whereas, Lloyd and Sparrow [1970] mainly focused on the transition on the heated plate facing upwards, but they provided experimental data of the critical Grashof number only at 10° for the heated plate facing downward.

Motivation of this study is therefore on the transition of free convection flow developing in a channel with the heated plate facing downward. Attention is restricted to the flow of air ($Pr = 0.7$)

with potential application linked to the convection occurring under a photovoltaic panel (e.g. see Wilson and Paul [2011]). Effects of the width and angle of the channel on the transition stage will also be examined under various air and plate temperatures by using the local values of velocity, turbulent kinetic energy and heat transfer.

2. GEOMETRY AND NUMERICAL MODELLING

The channel is formed by two inclined plates each with length L , and the distance between the plates is denoted by b . The wall on the top side is isothermal and heated below, while the other one is adiabatic. The numerical simulation is considered to be two-dimensional free convection and steady state. Air is chosen to be the test fluid. The model geometry along with the Cartesian coordinate system is shown in Figure 1.

The conservation equations of mass, momentum and energy for a two-dimensional incompressible fluid flow are respectively written in the following forms:

$$\frac{\partial(\rho u)}{\partial x} + \frac{\partial(\rho v)}{\partial y} = 0, \quad (1)$$

$$\frac{\partial(\rho uu)}{\partial x} + \frac{\partial(\rho uv)}{\partial y} = -\frac{\partial P}{\partial x} + \frac{\partial}{\partial x} \left(\mu \frac{\partial u}{\partial x} \right) + \frac{\partial}{\partial y} \left(\mu \frac{\partial u}{\partial y} \right) + g \sin \theta (\rho - \rho_0), \quad (2)$$

$$\frac{\partial(\rho vu)}{\partial x} + \frac{\partial(\rho vv)}{\partial y} = -\frac{\partial P}{\partial y} + \frac{\partial}{\partial x} \left(\mu \frac{\partial v}{\partial x} \right) + \frac{\partial}{\partial y} \left(\mu \frac{\partial v}{\partial y} \right) + g \cos \theta (\rho - \rho_0), \quad (3)$$

$$\frac{\partial(\rho u T)}{\partial x} + \frac{\partial(\rho v T)}{\partial y} = \frac{\partial}{\partial x} \left(\Gamma \frac{\partial T}{\partial x} \right) + \frac{\partial}{\partial y} \left(\Gamma \frac{\partial T}{\partial y} \right). \quad (4)$$

These equations are solved directly (subject to the boundary conditions described below) for the natural convection flow in the laminar region, while in the turbulent region both the “ μ ” and “ Γ ” terms are replaced by their effective values, μ_{eff} and Γ_{eff} , which are defined by $\mu_{eff} = \mu + \mu_t$ and $\Gamma_{eff} = \mu/Pr + \mu_t/\tilde{A}_t$ respectively. In the recent study, Alzwayi and Paul [2013] have examined that the Realizable k - ϵ turbulent model (Shih et al. [1995]) performs best in predicting the transition of the free convection flow over a vertical channel, compared to the other two well know models (standard and

RNG). Therefore, this model is particularly chosen in the present study to determine the turbulent viscosity μ_t which depends on the turbulent dissipation energy μ and the turbulent kinetic energy k .

No slip boundary condition is imposed on the velocity components at the both walls for which we set $u_i = 0$. The thermal boundary conditions for the heated and the adiabatic plate are defined as $T = T_p$ at $x = 0$ and $\frac{\partial T}{\partial x} = 0$ at $x = b$ respectively. Moreover, the turbulent kinetic energy vanishes at the walls so we set $k = 0$. Since distributions of the characteristics of the flow have large gradient near the walls, an enhanced wall function is also used in the wall boundary. Inlet boundary is subject to the ambient conditions, while at the outlet the static gauge pressure is set to zero.

The numerical methods used to solve the governing equations have already been described in Alzwayi and Paul [2013] and validated with suitable experimental data in a vertical heated channel. Moreover, an in-depth investigation on the grid resolution has also been carried out by using six different grids (22×220 , 30×370 , 120×370 , 200×370 , 300×370 and 200×400) with a fine resolution of mesh clustered near the inlet and the channel walls. The variation seen in the simulation results predicted by the last four grids is very small and almost negligible. The same agreement is received when we have tested these in the channel at an orientation angle of 45° . Therefore, as in the previous study, the grid size of 200×370 is chosen to avoid any undesirable discrepancies in the numerical results and at the same time to save the computational time to perform all the numerical simulations.

3. RESULTS AND DISCUSSION

3.1 EFFECT OF WIDTH AND ANGLE OF THE CHANNEL ON THE OUTLET PARAMETERS

Outlet velocity, temperature and average heat transfer are presented in this section to investigate the effects of the width and inclination angle of the channel on these parameters. The upper plate is kept isothermal at 70°C when the lower one is adiabatic, and the temperature of air is 15°C. The effect of the channel width (b) and its inclination (α) is first shown in Figure 2 on the normalised outlet temperature derived as $dT_{inc} = (T_{out} - T_{in})/T_{in} \times 100$. In general, the results show that the outlet temperature increases when the width of the channel is gradually reduced. But, the effect of the inclination angle is not straightforward and the temperature seems to have more influenced by the small width length of the channel (e.g. when $b \leq 0.15$ m) when it is particularly positioned at an angle greater than 60°. The gradual drop in the outlet temperature for the one-plate case with the angle indicates the effects of the free boundary which is subject to the ambient conditions. While, for the channel flow cases the adiabatic wall influences the development of the thermal boundary layers inside the channels.

The outlet velocity in Figure 3 also shows a general trend i.e. it increases as b is reduced. But, in contrast to the temperature, the flow velocity is reduced when the channel is moved from its vertical position due to an increase in the velocity component (u) acting in the horizontal direction (x) of the channel which in turn causes a drawback to the flow travelling downstream of the channel. In terms of quantifying the magnitude of the velocity drop, the channel with $b = 0.10$ m is selected, and we find that the velocity drops by about 20% from 10° to 50°, while it is about 50% from 50° to 80°. Therefore, the effect on the velocity is pronounced when the channel orientation is close to the horizontal position due to strong diffusion caused by the other velocity component as highlighted above.

Average heat transfer, $h = qp/(Tp - Ta)$, results are presented in Figure 4 in a bid to characterise the effects on the process of heat transfer occurring in the channels with varying both the width and orientation angle. Heat transfer in the vertical position is highest in magnitude compared to that in

other inclined positions, and the effect at higher inclination angles appears to be strong. This phenomenon is explained by the fact that when the channel is inclined at an angle to the vertical position, the buoyancy component exists in the direction into the heated surface as $g\beta''V\sin\theta$, where $\beta''V$ is the volume of the fluid displaced. The buoyancy component causes the pressure at the heated plate to be higher than that in the fluid which further causes an outward flow away from the heated surface. The thermal boundary layer growth is then affected by this process, and as a result the heat transfer between the plates and fluid falls. While in the vertical case the buoyancy component acts only in the flow direction (as given by $g\beta''V$), and the heat transfer is therefore predicted to be maximum. However, an interesting but rather complex effect is found while varying the width b . Starting from the single plate case, when the width of the channel is reduced to 0.3 m, the average heat transfer increases moderately. But, a sudden drop is predicted for $b = 0.2$ m and the heat transfer increases again when the width is reduced to 0.15m followed by a systematic growth as b is reduced further. This variation is clearly seen in Figure 5 where the same results are plotted but against the channel width. All the curves show a sudden deep near at $b = 0.2$ m. It is understood from this phenomenon that when the width of the channel $b \leq 0.2$ m, the development of convection flow inside the channel is constrained by the small gap available between the plates, which causes the average heat transfer to decrease and it becomes a minimum at $b = 0.2$. While, the larger channel width allowed the convection flow to develop rapidly inside the channel and the result is that the heat transfer coefficient increases with the width until the effect of the presence of the adiabatic plate disappears slowly. We also note that the behaviour reported in the heat transfer coefficient shows a very good agreement qualitatively with the experimental data of Onur et al. [1997] and Baskaya et al. [1999]. Onur et al. [1997] explained that the fluid largely remains motionless due to frictional forces retarding the development of natural convection when the plate spacing is relative small. Heat transfer decreases with an increase in the plate spacing to a minimum until the frictional losses is minimised. However, a further increase in the spacing causes acceleration in fluid motion and, as a result of this, the rate of heat transfer increases.

3.2 EFFECT OF ORIENTATION ANGLE ON THE TRANSITION STAGE

In this section, transition behaviour of the air flow is presented with the channel inclination for the width of $b = 0.08$ m and 0.10 m. The first set of results pertains to present the distributions of the maximum velocity and kinetic energy in Figure 6 determined by using $f_{\max}(y) = \underset{x \min \leq x \leq x \max}{Max} f(x, y)$, where f is a generic function, and plotted along the vertical axis y . Figures 6(a) and (c) show typical results of the velocity profiles along the channel, e.g. the velocity gradually grows from the inlet and reaches its maximum at the point where the flow transition occurs. However, the velocity magnitude drops slightly after the transition and becomes almost steady towards the outlet. Particularly, when $\theta = 30^\circ$ the velocity profiles increase slightly in the region close to the outlet which has a good agreement with the results of Said et al. (2005b).

The turbulent kinetic energy (Figures 6(b, d)), on the other hand, has zero values within the laminar region of the flow, which then grows rapidly from a location where the process of transition begins with a steady growth within the whole transition region. A sharp increase is followed in the most cases within the region of the turbulent flow. In case of $b = 0.08$ m and when $\theta = 50^\circ$ the kinetic turbulence energy grows slightly after the transition point and then increases sharply in the rest of the region as seen in Figure 6(b). This is further clarified in the contour plots in Figures 7 (A) and (B), where the growth of the turbulent kinetic energy inside the channel is presented. As seen, the turbulent kinetic energy grows early on the adiabatic plate, particularly when the channel width is reduced. The phenomena are explained by the fact that though the flow is accelerated rapidly near the heated plate, as evidence by the rising velocity peak beside the heated plate shown in Figure 8 for $b = 0.08$ m, the magnitude of the velocity adjacent to the opposite adiabatic plate drops which causes a flow deceleration and results in an increase of the turbulent kinetic energy near the adiabatic surface. However, we note that when the width of the channel is systematically increased, the velocity profiles show less deceleration effects on the flow and hence the turbulent kinetic

energy appears to spread to a wide range of the channel. We further note that the behaviour reported in the production of the turbulent kinetic energy inside the channel show good qualitative agreement with the experimental data of Katoh et al. (1991) and Yilmaz and Fraser [2007].

The second set of result pertains to the distributions of local heat transfer along the heated plate for all the inclination angles and for $b = 0.08$ and 0.10 m. Figure 9 generally shows that the local heat transfer is much higher at the edge of the channel near the inlet than that of the downstream due to a larger temperature difference occurred between the heated plate and the air flow with a thinner thermal boundary layer developing at the upstream than that at the downstream. However, the thermal boundary layer gets fatter along the heated plate which causes a rapid decrease in the local heat transfer until it again starts to grow slowly after the transition stage. In particular, the growth of the local heat transfer after the transition becomes sharp for $b = 0.10$ m compared to $b = 0.08$ m due to the possible fact that there is no enough space available for the thermal boundary layer to fully develop in the channel. Moreover, a systematic increase in the tilting angle causes the transition point to move further downstream; as a result the turbulent region at a particularly higher orientation angle becomes relatively short. In addition, the local heat transfer just prior to the outlet section increases slightly for $\theta \leq 30^\circ$ due to an increase seen in the velocity near the outlet (Figure 6).

Since the peak of the velocity distributions from the heated plate can be considered to be a starting point of the transition stage and according to Katoh et al. [1991] the location of a minimum point of the local heat flux should also correspond to the transition point, the three different parameters such as the heated air velocity, turbulent kinetic energy and local heat flux are used to predict the critical distance (L_c) of the flow in the channel and summarised in Figures 10 (a) and (b) respectively, for $b = 0.08$ m and 0.10 m. In general, as the inclination of the channel is increased, the critical distance predicted by all the three parameters increases, indicating a late transition due to the stable convection flow inside the channel. Notably, further the channel from the vertical position, the

predicted critical distances by the velocity and turbulent kinetic energy are very close to each other. In the channel, with a small width e.g. $b = 0.08$ m (Fig. 10a), the critical distance predicted by the heat flux is less than the other two parameters when $\beta \leq 50^\circ$, and it is approximately half when $\beta \leq 10^\circ$. But, when the angle is increased the critical distance increases sharply and shows an over prediction with those obtained by the velocity and turbulent kinetic energy when $\beta \leq 70^\circ$.

The structure of the flow within the boundary layer and the behaviour of the flow near the surface are very important factors affecting the transport of the energy and mass in the transition stage. That is why, the critical distance indicating the transition of the flow was estimated by the velocity, kinetic energy and heat flux plate as presented in Figure 10. In order to understand the effect of the angle of the plate on the distribution of the velocity and the temperature of the air flow, both of them are presented against x in Figure 11 at $y = 0.5$ m, 1.5 m and 3.0 m. The velocity magnitude generally drops with an increase in the angle in all the cases and the peak moving far away from the heated plate. Likewise, the thickness of the thermal boundary layer also drops with the angle, especially when $\beta \leq 70^\circ$ (frames c, i and h). But, an increase in the air temperature beside the heated wall is caused by the buoyancy force component acting normal to the surface. This buoyancy force also affects the transition process with a delay in the separation of the sub-layers from the heated surface, causing a much higher velocity gradient close to the adiabatic wall with an occurrence of the backflow predicted at the far downstream besides the adiabatic wall when $\beta \leq 70^\circ$ (see frames c, f, i and m).

3.3 EVALUATION OF THE TRANSITION STAGE

In this section, comparison of the numerical predicted results with various experimental data is made on the critical Grashof number derived from $Gr_c = g\beta(T_p - T_\infty)Lc^3/\nu^2$ at the critical distance (Lc) as described in §3.1. Comparison in Figure 12 shows that our numerical results for the one heated plate case have very good agreement with the experimental data of Lloyd and Sparrow

[1970] at $\beta = 0^\circ$ and 10° . While the result of Hassan and Mohamed [1970] clearly under-predicted the critical Grashof number compared to Lloyd and Sparrow [1970]. AL-Arabi and Sakr [1988] reported the results at the start and end of transition (filled circle and square respectively), and our results show good agreement with the former data while under-predict against the latter data. Tritton [1963], on the other hand, paid particular attention to the vertical and inclined ($\beta = 50^\circ$) plates heated both above and below. He found $Gr_c = 9.26 \times 10^6$ on the vertical plate (not shown in this figure), which clearly falls very much compared to the other experimental data presented in Figure 12. This under-prediction occurred due to the effects of the strong disturbances in the laboratory room and the uncertainty into the evaluation of the vertical critical distance, as mentioned by Tritton himself. We also note here that no other suitable data are available for the other orientation angles; therefore it is not possible for us to compare the results at higher angles. Moreover, in the case of channel with the heated surface facing downward, very little information is available in the literature and the transition data are unavailable to make any comparison against the simulated critical Grashof numbers for various b . But the results, already presented in Figure 10 for $b = 0.08$ m and 0.10 m, show satisfactory agreement in the critical distance estimated by using the three different physical quantities.

Critical Grashof numbers for other values of the channel width from $b = 0.06$ m to 0.30 m are also shown in Figure 12 at a wide range of the inclination angle. With a small increase in the channel width from $b = 0.06$ m to 0.08 m, the critical Grashof number increases which again suggests a late transition of the flow. Variation in the transition point appears to be almost steady until the channel is nearly horizontal. However, further increase in the channel width from 0.08 m to 0.30 m causes an early transition and, as a result the critical Grashof number increases gradually first with the inclination angle and then rapidly when $\beta \geq 50^\circ$. In fact, for the single heated plate case facing downward a ten-fold increase in the critical Grashof number is predicted when it is inclined at $\beta = 85^\circ$ from the vertical position.

3.4 EFFECT OF TEMPERATURE OF AIR AND PLATE ON THE TRANSITION STAGE

In this section, following variations in the temperature of air and heated plate have been examined 15°C, 25°C, 30°C and 70°C, 90°C, 100°C respectively, for $b = 0.10$ m and 0.20 m. The main objective here is to investigate the effects of the buoyancy force, which is generated by the difference of the flow density as a result of the air and plate temperatures, on the transition stage. Numerical results are summarised in terms of the critical Grashof number, $Gr_c = g\beta(T_P - T_a)L_c^3/\nu^2$, determined from the critical distance (L_c) and presented in Figure 13. Note that when the air temperature (T_a) was varied we kept the plate temperature fixed at $T_P = 70^\circ\text{C}$, while the air temperature was fixed at $T_a = 15^\circ\text{C}$ for the variation of the plate temperature. It can be seen in this figure that the critical Grashof number generally increases with the orientation angle irrespective to the variation in the temperature and the channel width. In fact, we find about a ten-fold increase in the magnitude of the critical Grashof number when the channel is rotated from its vertical to a nearly horizontal position. Therefore, it can be concluded again that the transition becomes late when the channel is moved from the vertical position.

In terms of the variation of both the plate and air temperatures, a very little effect is found on the critical Grashof number when $\theta \leq 50^\circ$. While at a relatively large angle (e.g. when $\theta > 50^\circ$) the effect found is more pronounced for $b = 0.10$ m (frame a) than $b = 0.20$ m (frame b). Specifically, the results in frame (a) show that the critical Grashof number for the cases with $\theta > 50^\circ$ drops when the air temperature is increased from 15°C by fixing the plate temperature to 70°C. This behaviour further illustrates the flow becoming unstable at the early stage of the transition process. However, increasing the plate temperature shows an opposite effect, again resulting in a late transition with more stable flow at a higher orientation angle. In the case of higher channel width (frame b), as already mentioned, variation on the air temperature seems to have a moderate effect on the critical Grashof number than the plate temperature when $\theta > 50^\circ$.

4. CONCLUSION

Effects of inclination angle of the parallel-plate channel and its width on the developing free-convection flow have been investigated numerically under various operating and geometrical conditions. For example, the inclination angle was varied from 0° to 85° from the vertical position when the distance separating the two parallel plates was systematically reduced from 0.045 m to 0.06 m.

Results presented show that the average of heat transfer coefficient depends on both the width and angle of the channel. Fixing the channel inclination and increasing the channel width from 0.06m, we find that the heat transfer coefficient initially drops to a minimum value, followed by increment at a large width. This effect becomes very small when the adiabatic plate is located relatively at a far distance apart. However, when the angle of the channel is over 70° , the thickness of both the thermal and velocity boundary layers drop sharply due to the flow intensity increased especially around the middle of the channel, resulting an increased outlet temperature.

At the transition stage, the results also show that both the width and inclination of the channel have major effects. For example, as the inclination angle is increased, the transition stage moves further downstream of the channel. The critical distance predicted by both the velocity and turbulent kinetic energy agree very well, while it is slightly over-predicted by the local heat flux as a result of the buoyancy force increasing to the normal of the heated plate. Good agreement is obtained while compared the critical Grashof number with various experimental data. Moreover, different values of the air and plate temperature are used to examine the transition stage in the channel.

REFERENCES

- AL-Arabi, M. and Sakr, B. [1988], Natural convection heat transfer from inclined isothermal plates, *International Journal of Heat and Mass Transfer*, Vol. 31, pp 559-566.
- Alzwayi, A.S. and Paul, M. C. [2013], Effect of width and temperature of a vertical parallel plate channel on the transition of the developing thermal boundary layer, *Int. J. Heat Mass Transfer*, <http://dx.doi.org/10.1016/j.ijheatmasstransfer.2013.03.056>, v63, pp20-30.
- Azevedo, L. F. A. and Sparrow, E. M. [1985], Natural convection in open - ended inclined channels, *International Journal of Heat Transfer*, Vol.107, pp 893-901.
- Balck, W. Z. and Norris, J. K. [1975], The thermal structure of free convection turbulence from inclined isothermal surfaces and its influence heat transfer, *International Journal of Heat and Mass Transfer*, Vol. 18, pp 43-50.
- Baskaya, S. Aktas, M. K. and Onur, N. [1999], Numerical simulation of the effects of plate Separation and Inclination of heat transfer in buoyancy driven open channels, *Heat and Mass Transfer*, Vol. 35, pp 273-280.
- Elenbaas, W. [1942], Heat dissipation of parallel plates by free convection, *Physica IX* 9, pp 1-28.
- Fedorov, A. G. and Viskanta, R. [1997], Turbulent natural convection heat transfer in an asymmetrically heated vertical parallel-plate channel, *International Journal of Heat Mass Transfer*, Vol. 40, pp 3849-3860.
- Hassan, k. and Mohamed, S. A. [1970], Natural convection from isothermal flat surfaces,

International Journal of Heat and Mass Transfer, Vol. 13, pp 1873-1886.

Kato, Y. Miyamoto, M. Kurima, J. and Kaneyasu, S. [1991], Turbulent free convection heat transfer from vertical parallel plates, *JSME International Journal*, Vol. 34, pp 496-501.

Kierkus, W. T. [1968], An analysis of laminar free convection flow and heat transfer about an inclined isothermal plate, *International Journal of Heat and Mass Transfer*, Vol. 11, pp 241-253.

Lloyd, R. J. and Sparrow, E. M. [1970], On the instability of natural convection flow on inclined plates, *Journal of Fluid Mechanics*, Vol. 42, pp 465-470.

Manca, O. Nardini, S and Naso, V. [1992], Experimental analysis of natural convection in a tilted channel, *11th Australasian Fluid Mechanics Conference*, University of Tasmania, Hobart, Australia, pp 131-134.

Markatos, N, C. and Pericleous, K, A. [1984], Laminar and turbulent natural convection in an enclosed cavity, *International Journal of Heat and Mass Transfer*, Vol. 27, pp 755-772.

Miyamoto, M. Kato, Y. and Kurima, J. [1983], Turbulent free convection heat transfer from vertical Parallel plates in air, *NII - Electronic Library service, the Japan Society of Mechanical Engineers*, Vol. 34, pp 1-7.

Onur, N. and Aktas, M. K. [1998], An experimental study on the effect of opposing wall on natural convection along an inclined hot plate facing downward, *International Communications in Heat and Mass Transfer*, Vol. 25, pp 389-397.

- Onur, N. Sovrioglu, M. and Aktas, M. K. [1997], An experimental study on the natural convection heat transfer between inclined plates (lower plate isothermally heated and the upper plate thermally isolated as well as unheated), *Heat and Mass Transfer*, Vol. 32, pp 471-47.
- M. C. Paul, D. A. S. Rees & M. Wilson [2005], “The influence of higher order effects on the vortex instability of thermal boundary layer flow in a wedge-shaped domain” *International Journal of Heat and Mass Transfer*, vol 48, no 8, pp1417-1424.
- Rich, R. B. [1953], An investigation of heat transfer from an inclined flat plate in free convection, *International Journal of Heat and Mass Transfer*, Vol. 11, pp 241-25.
- Said, S. A. M., Habeb, M. A. and Anwar, [2005a], Turbulent natural convection between inclined isothermal plates, *Computer and Fluids*, Vol. 34, pp 1025-1039.
- Said, S. A. M. Habeb, A. Badr, H. M. and Anwar, S. [2005b], Numerical investigation of natural convection inside an inclined parallel walled channel, *International Journal for Numerical Methods in Fluids*, Vol. 49, pp 569-582.
- Shih, T. H. Liou, W. W. Shabbir, A. Yang, Z. and Zhu, J. [1995], A new $k - \mu$ eddy viscosity model for high Reynolds number turbulent flows, *Computers and Fluids*, Vol. 24, pp 227-238.
- Tritton, D. J. [1963], Transition to turbulence in the free convection boundary layers on an inclined heated plate, *Journal of Fluid Mechanics*, Vol. 16, pp 417-435.
- Wilson, M. J. and Paul, M. C. [2011], Effect of mounting geometry on convection occurring under a photovoltaic panel and the corresponding efficiency using CFD, *Solar Energy*, v85, pp2540-50.

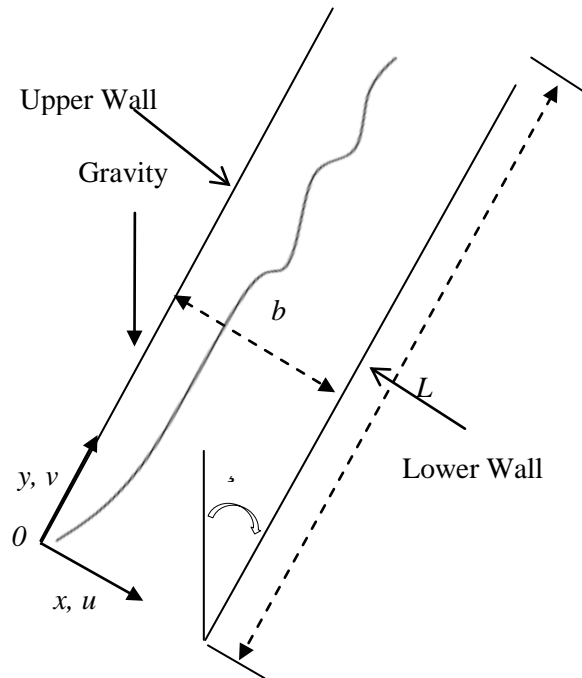


Figure 1. Flow geometry with coordinate directions.

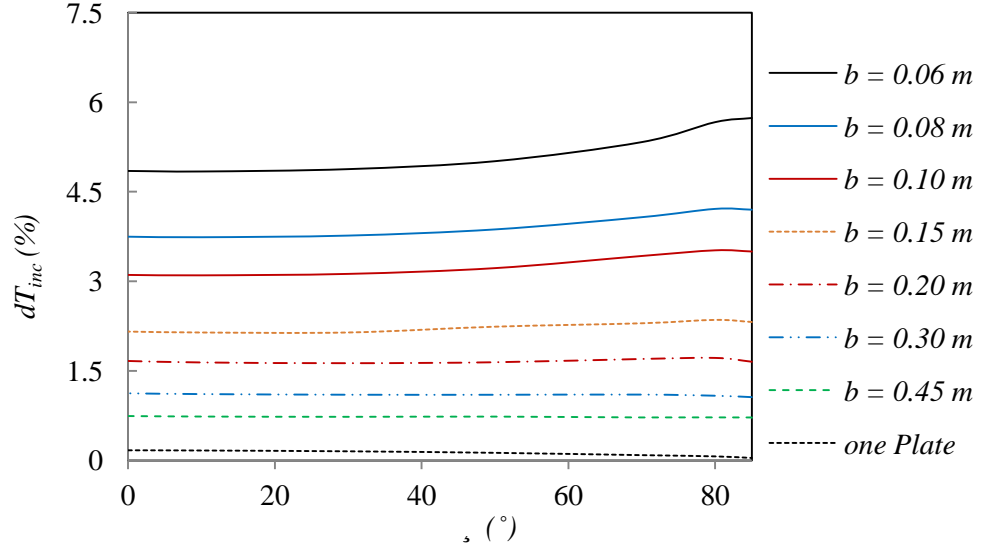


Figure 2. The average outlet temperature at $Ta = 15^\circ\text{C}$ and $Tp = 70^\circ\text{C}$.

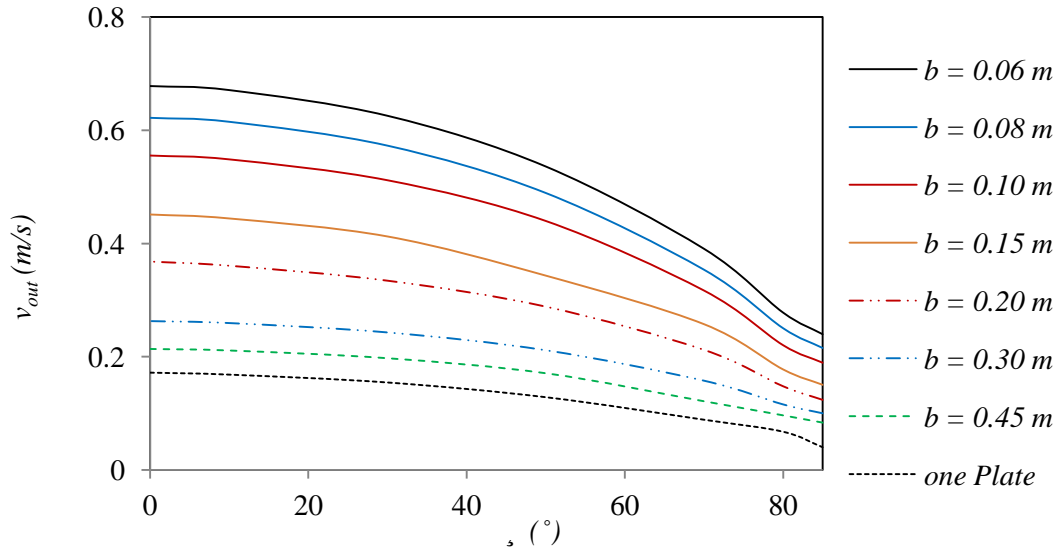


Figure 3. The average outlet velocity at $Ta = 15^\circ\text{C}$ and $Tp = 70^\circ\text{C}$.

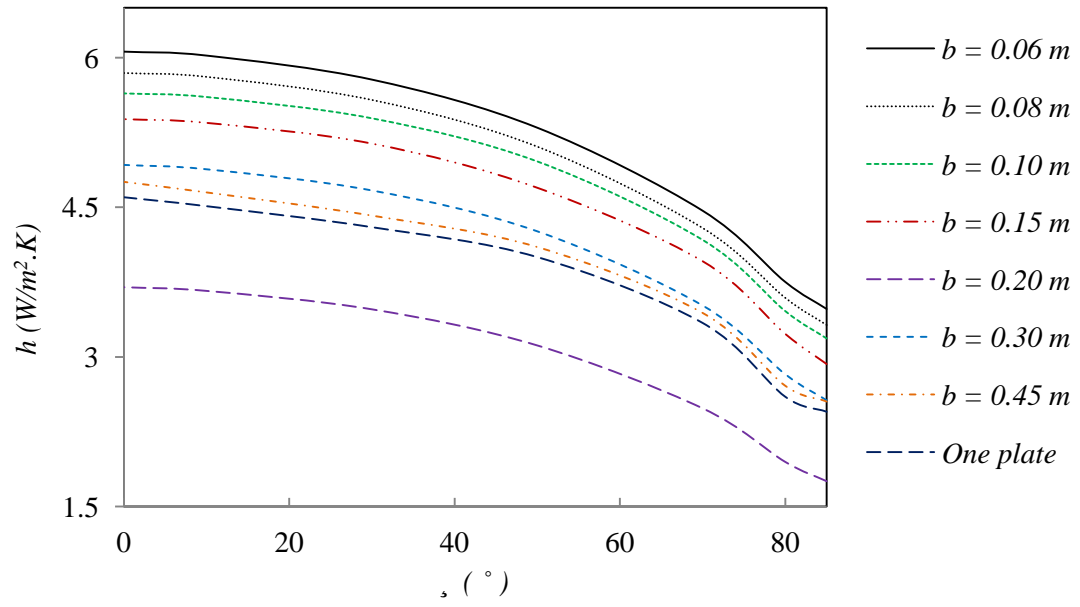


Figure 4. Effect of the channel width on the average heat transfer at $Ta = 15^{\circ}\text{C}$ and $Tp = 70^{\circ}\text{C}$.

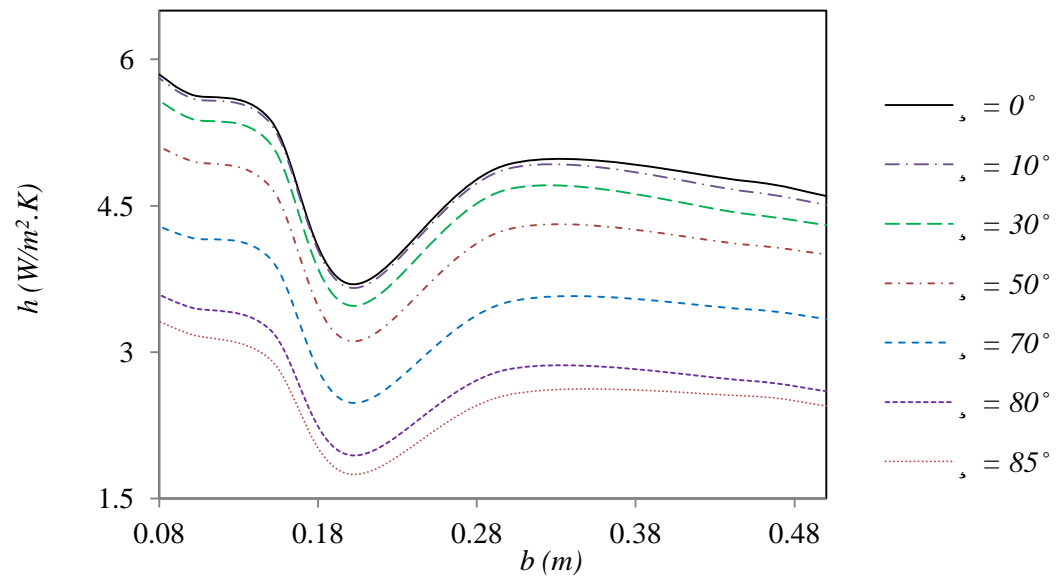


Figure 5. Effect of the inclination angle on the average heat transfer at $Ta = 15^{\circ}\text{C}$ and $Tp = 70^{\circ}\text{C}$.

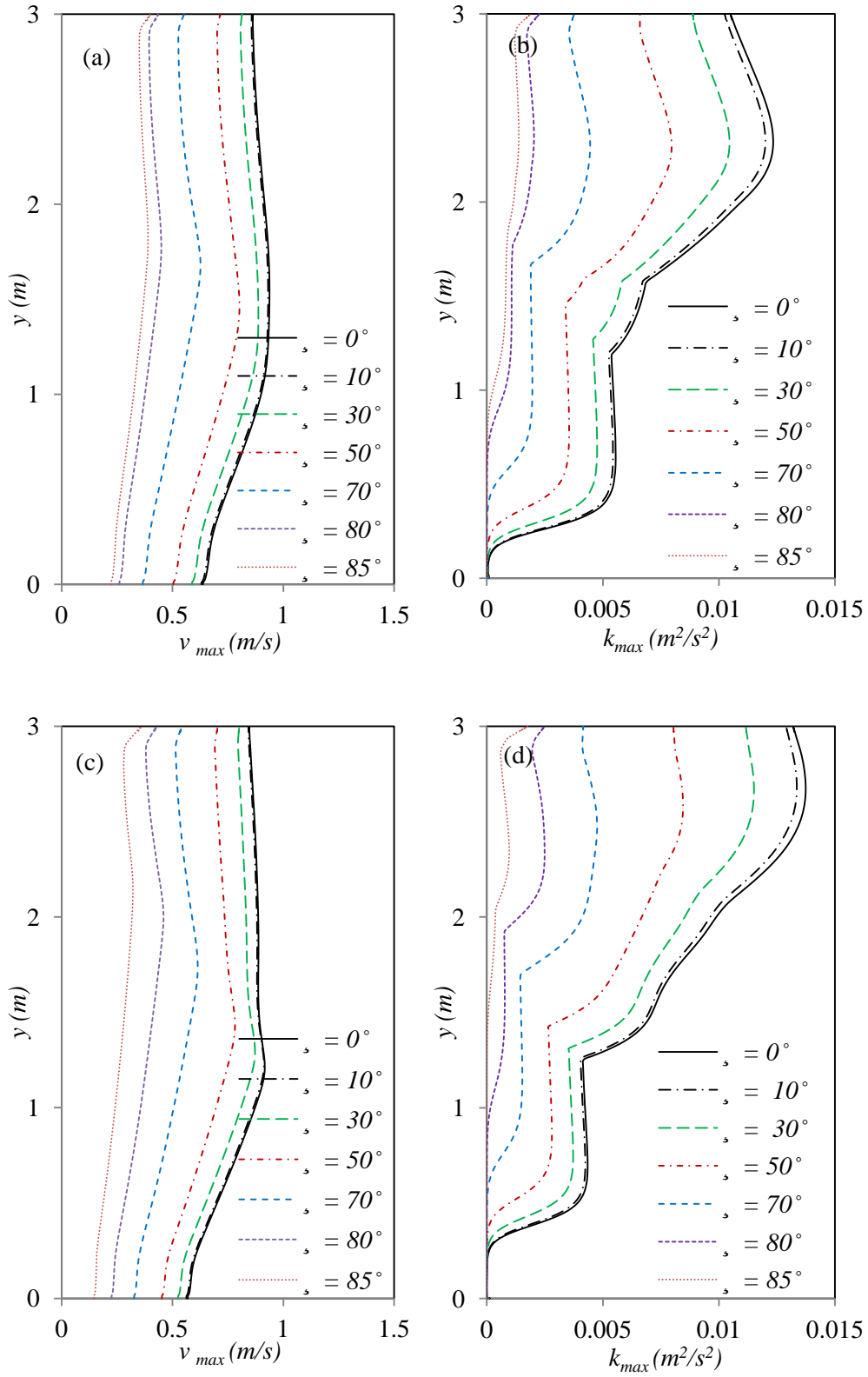


Figure 6. Distributions of the maximum velocity and turbulent kinetic energy for $b = 0.08$ m (a, b) and $b = 0.10$ m (c, d) at $Ta = 15^\circ\text{C}$ and $Tp = 70^\circ\text{C}$.

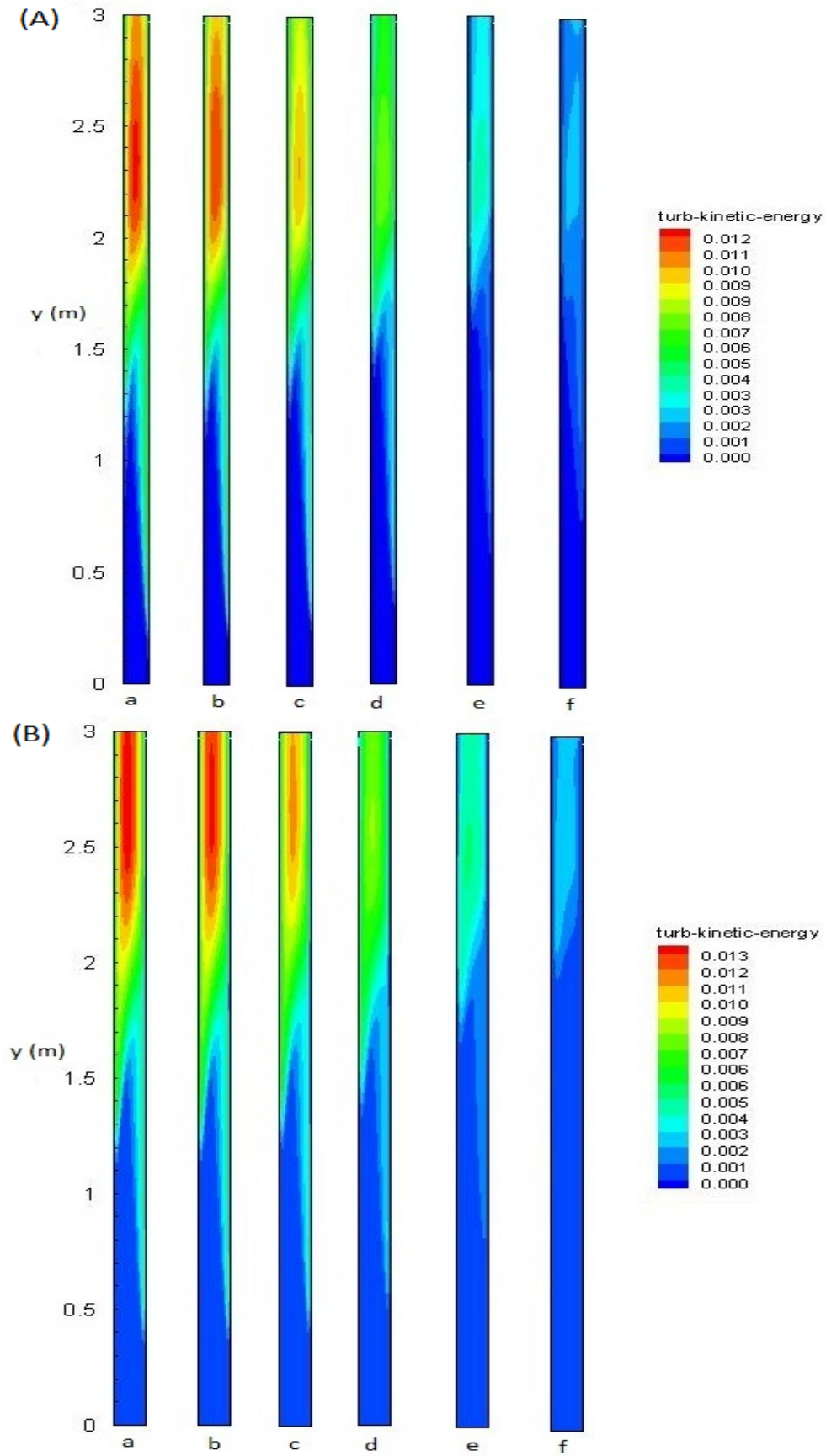


Figure 7. Contours of the turbulent kinetic energy, where the width of the channel is (A) 0.08 m and (B) 0.10 m and the angle θ is (a) 0°, (b) 10°, (c) 30°, (d) 50°, (e) 70° and (f) 85°.

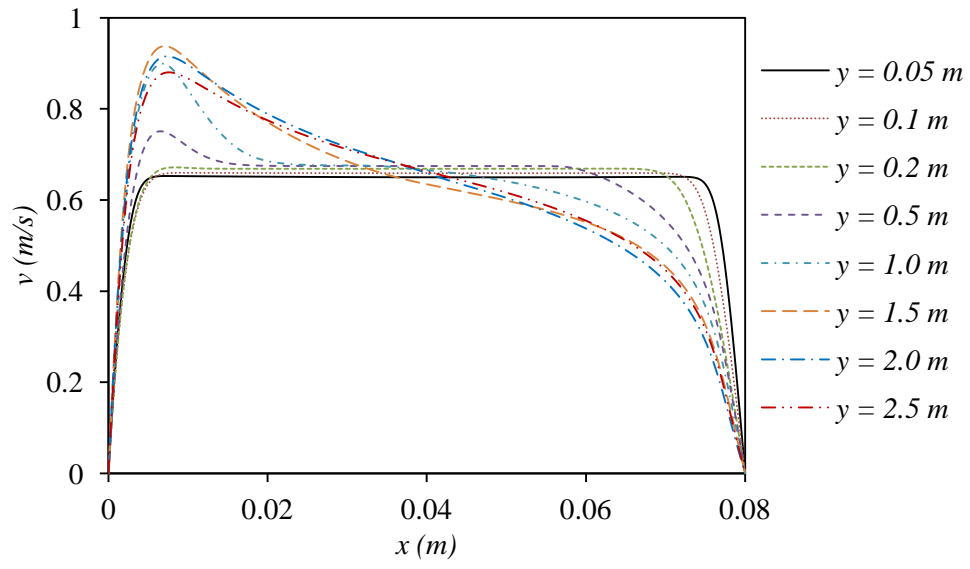


Figure 8. The distribution of velocity inside the channel for $b = 0.08$ m.

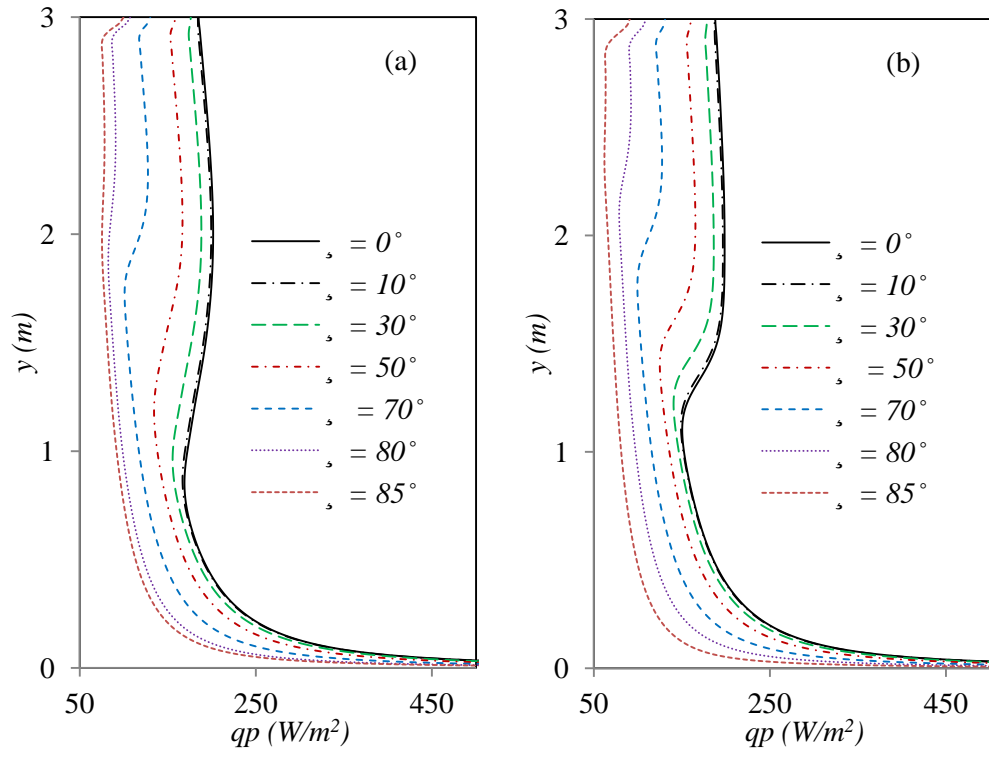


Figure 9. The distribution of the local heat transfer for (a) $b = 0.08$ m and (b) $b = 0.10$ m.

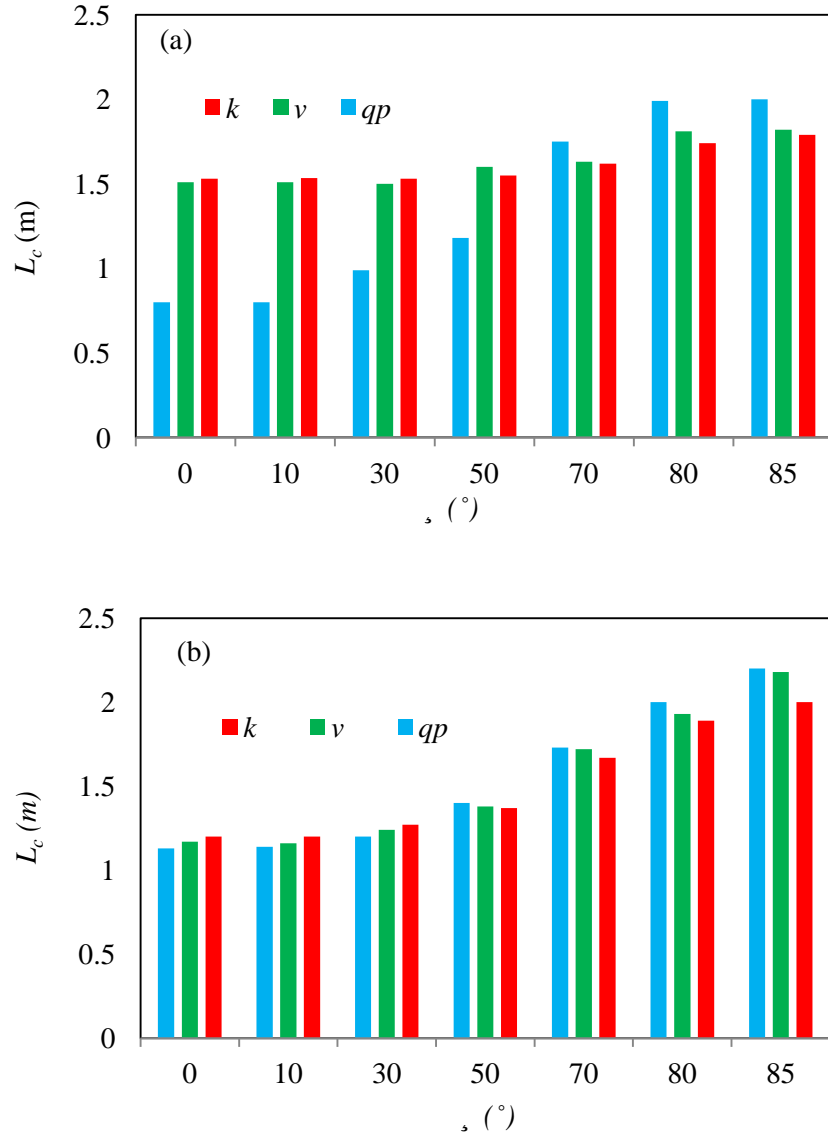


Figure 10. The critical distance derived from the velocity, turbulent kinetic energy and plate heat flux for (a) $b = 0.08$ m and (b) $b = 0.10$ m.

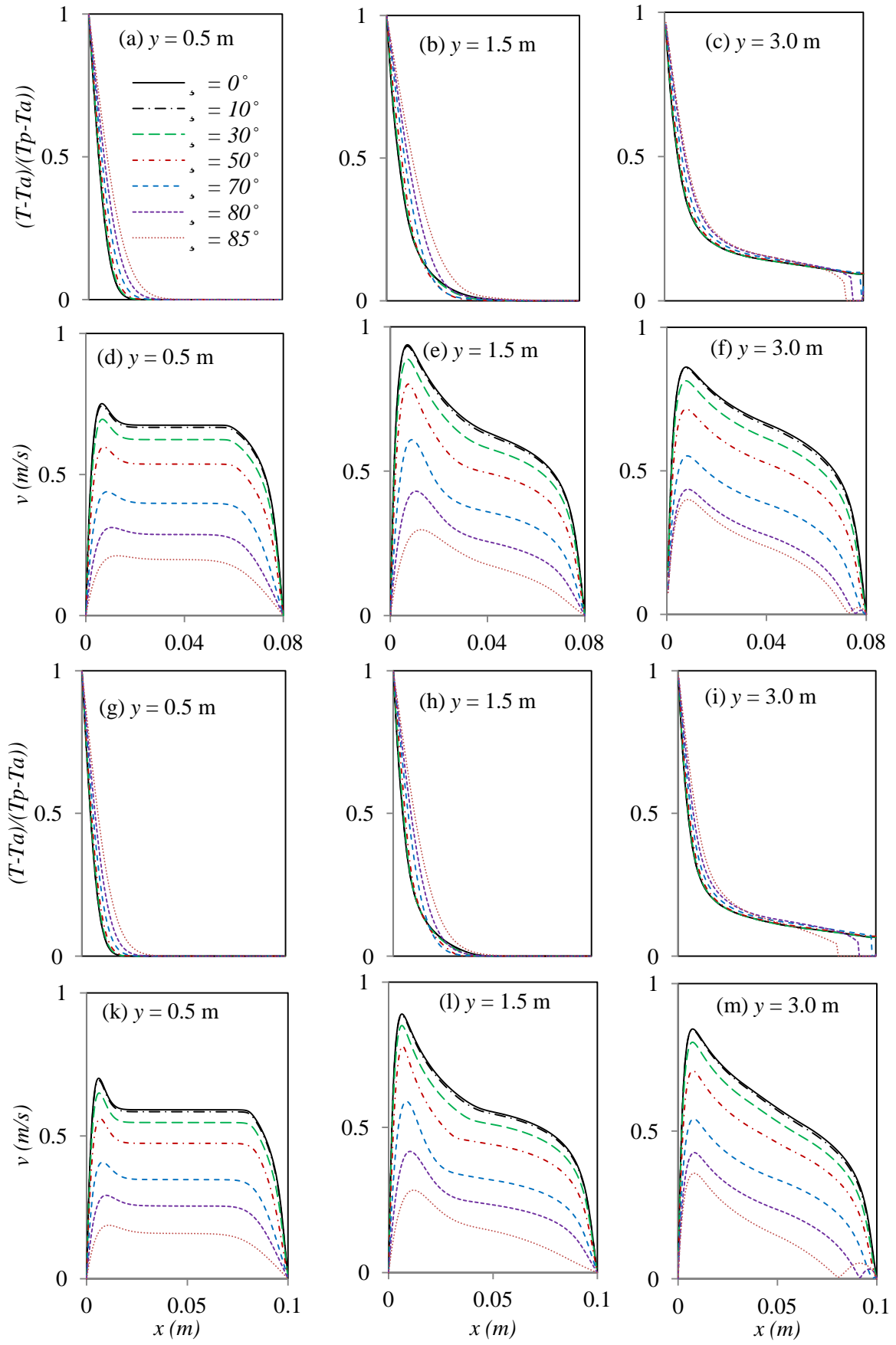


Figure 11. The distributions of the temperature and velocity where (a–f) for $b = 0.08$ m and (g–m) for $b = 0.10$ m.

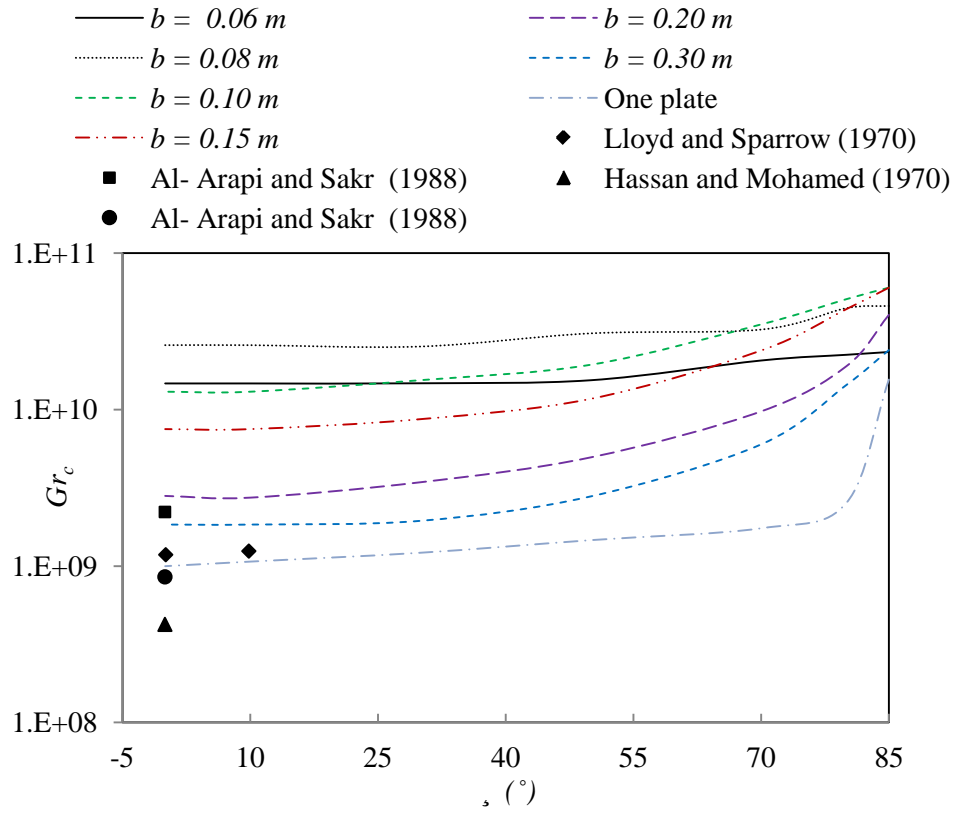


Figure 12. The critical Grashof number derived at different inclination angles and b .

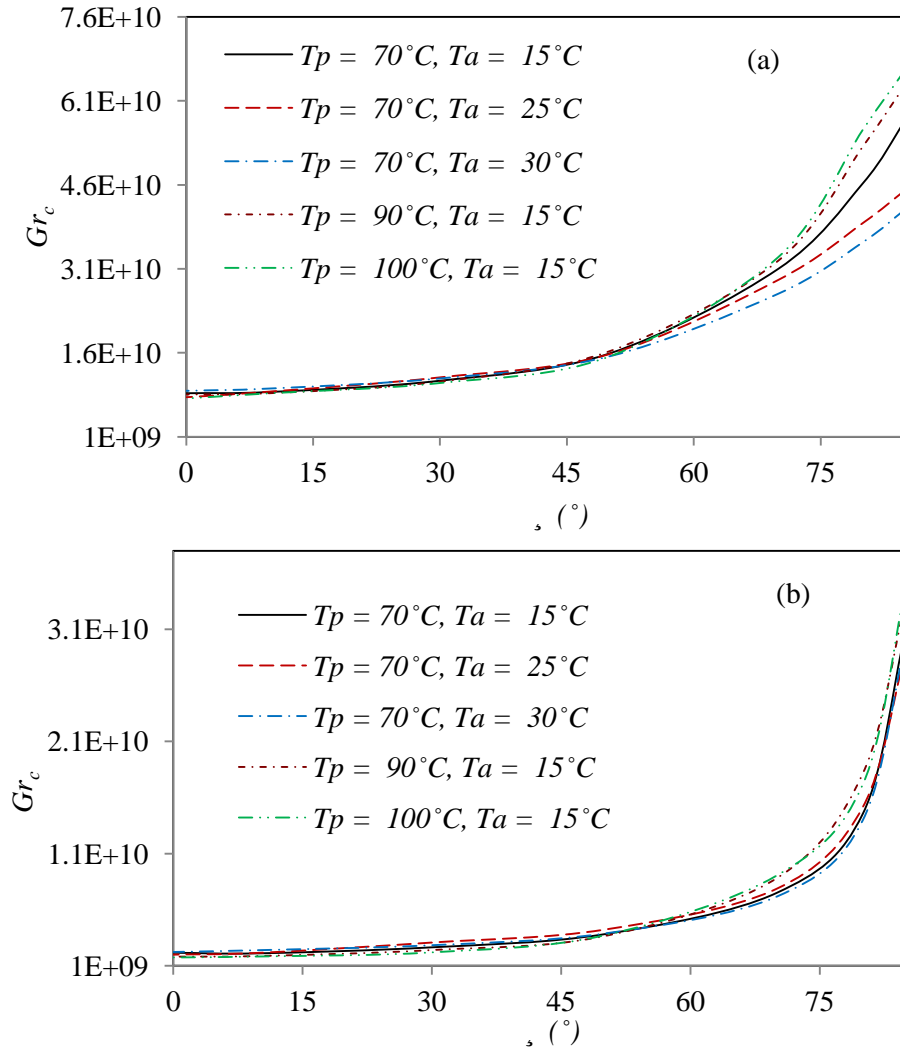


Figure 13. Critical Grashof number on the heated plate for (a) $b = 0.10$ m and (b) $b = 0.20$ m